Structure, Vol. 13, 213–223, February, 2005, ©2005 Elsevier Ltd All rights reserved. DOI 10.1016/j.str.2004.11.013

Solution Structure of the Tctex1 Dimer Reveals a Mechanism for Dynein-Cargo Interactions

Hongwei Wu, Mark W. Maciejewski, Sachiko Takebe, and Stephen M. King*
Department of Molecular, Microbial, and Structural Biology
263 Farmington Avenue
Farmington, Connecticut 06030

Summary

Tctex1 is a light chain found in both cytoplasmic and flagellar dyneins and is involved in many fundamental cellular activities, including rhodopsin transport within photoreceptors, and may function in the non-Mendelian transmission of *t* haplotypes in mice. Here, we present the NMR solution structure for the Tctex1 dimer from *Chlamydomonas* axonemal inner dynein arm I1. Structural comparisons reveal a strong similarity with the LC8 dynein light chain dimer, including formation of a strand-switched β sheet interface. Analysis of the Tctex1 structure enables the dynein intermediate chain binding site to be identified and suggests a mechanism by which cargo proteins might be attached to this microtubule motor complex. Comparison with the alternate dynein light chain rp3 reveals how the specificity of dynein-cargo interactions mediated by these dynein components is achieved. In addition, this structure provides insight into the consequences of the mutations found in the *t* haplotype forms of this protein.

Introduction

Dyneins are microtubule-based molecular motors that are involved in a wide variety of fundamental cellular activities. In the cytoplasm, dyneins power the retrograde trafficking of many components, including endosomes and lyzosomes, and they also are required for Golgi maintenance, breakdown of the nuclear envelope, and mitosis. Within flagella and cilia, dyneins are necessary for organelle assembly as they function as the retrograde intraflagellar transport motor and form the arms attached to the axonemal doublet microtubules that generate specific ciliary/flagellar waveforms (see Sakato and King, 2004 for a recent review). In mammals, defects in cytoplasmic dynein result in motor neuron disease (Hafezparast et al., 2003), whereas axonemal dynein mutations lead to a wide variety of defects, including immotile sperm, bronchial problems, and *situs inversus* (Afzelius, 1979).

In general, most dyneins have a mass of 1–2 MDa and consist of 2–3 heavy chains (~520 kDa each) that contain the ATPase and motor sites associated with a series of accessory components, including WD-repeat intermediate chains and three distinct classes of light chains (the LC8, Tctex1, and LC7/Roadblock families) that are involved in dynein assembly, cargo attachment, and perhaps regulation. Some dyneins also contain additional components such as the light intermediate chains (~53–57 kDa) found in the cytoplasmic isoforms or the regulatory light chains that are directly associated with individual motor units within outer arm dynein (see Sakato and King, 2004 and King, 2002 for recent reviews).

Tctex1 was originally described as a small gene family within the murine *t* complex (a 30–40 Mb region of chromosome 17) and is a candidate for one of the sterility/distorter factors involved in causing non-Mendelian segregation (so-called transmission ratio distortion or meiotic drive; see [Lyon, 2003] for a review) of variant forms of this chromosomal region known as the *t* haplotypes (Lader et al., 1989). Subsequently, Tctex1 was identified using biochemical and immunological methods as an integral component of the cytoplasmic dynein complex (King et al., 1996b). Tctex1 is present at a stoichiometry of two copies per motor particle (King et al., 1996b), and it indeed exists as a dimer (DiBella et al., 2001). In mammals, a second member of this protein family (originally termed rp3 [Roux et al., 1994]) that exhibits 55% sequence identity with Tctex1 is also a cytoplasmic dynein component that is differentially expressed in a cell-, tissue-, and developmentally regulated manner (King et al., 1998). Murine Tctex1 is also present in sperm (Harrison et al., 1998; Lader et al., 1989; O'Neill and Artzt, 1995), and closely related proteins have been found in axonemal dyneins from *Chlamydomonas* (Harrison et al., 1998) (L.M. DiBella and S.M.K., unpublished data) and sea urchin sperm flagella (Kagami et al., 1998). These observations, together with the identification of additional candidate distorters as flagellar dynein components, have led to the suggestion that defects in dynein function and sperm motility underlie the *t* haplotype chromosome segregation phenotype (Fossella et al., 2000; Harrison et al., 1998; Patel-King et al., 1997). Interestingly, in *Drosophila*, Tctex1 is not required for essential cytoplasmic dynein activities, but it is necessary for male fertility (Caggese et al., 2001; Li et al., 2004).

In addition to the dynein intermediate chain, cytoplasmic Tctex1 has also been found to associate with a wide variety of cellular components, including rhodopsin (Tai et al., 1999), Doc-2 (Nagano et al., 1998), various receptors—e.g., polio virus receptor CD155 (Mueller et al., 2002) and parathyroid hormone receptor (Sugai et al., 2003)—the voltage-dependent anion channel (Schwarzer et al., 2002), *Herpes* virus capsid protein VP26 (Douglas et al., 2004), and Fyn kinase (Kai et al., 1997; Mou et al., 1998). Interaction with Tctex1 is thought to mediate the attachment of these proteins to the dynein motor and thus allow for vectorial intracellular transport. For example, within the vertebrate photoreceptor, rhodopsin must be trafficked to the base of the connecting cilium prior to insertion into the membrane stacks. Several human mutations that result in *retinitis pigmentosa* occur very close to the C terminus of rhodopsin and cause a reduction in the binding affinity for Tctex1 (Tai et al., 1999). Importantly, the rp3 light chain does not bind rhodopsin, indicating that cytoplasmic dyneins with distinct light chain content can exhibit target binding specificity.

*Correspondence: steve@king2.uchc.edu

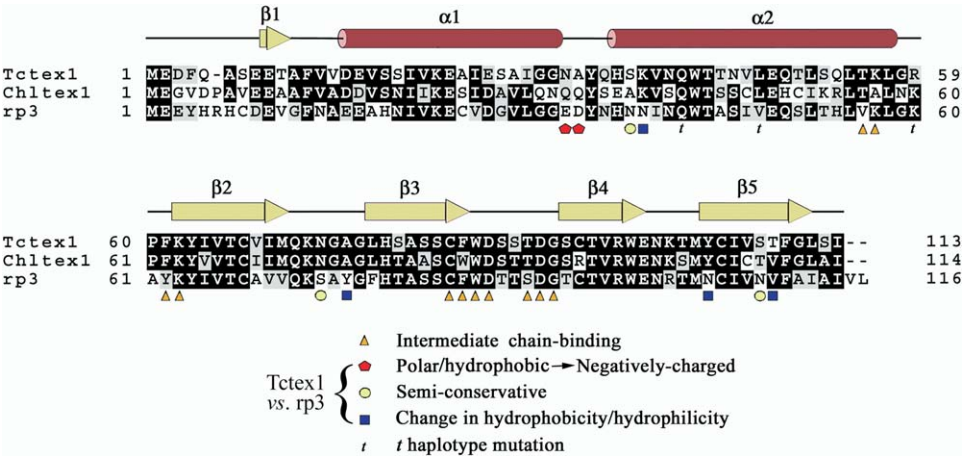

Figure 1. Sequence Alignment and Secondary Structure of Tctex1 Light Chains

Alignment of *Chlamydomonas* Tctex1 (*Chltex1*; T07930), murine Tctex1 (*Tctex1*; NP033368), and human rp3 (*rp3*; U02556) was performed using CLUSTALW and was processed with BOXSHADE. The secondary structure determined for *Chlamydomonas* Tctex1 is shown above the alignment. Note that the numbering of the β strands differs from that employed previously for the mammalian isoform (Mok et al., 2001). Residues indicated by an orange triangle show an alteration in chemical shift upon addition of an 11-residue dynein intermediate chain peptide (Mok et al., 2001). Other marked residues designate significant differences between Tctex1 and rp3 that may account for cargo binding specificity: red pentagon, polar or hydrophobic to negatively charged; yellow circle, semiconservative; blue square, large change in hydrophobicity/hydrophilicity. The three residues mutated in the *t* haplotype variants of murine Tctex1 are marked by "*t*."

To gain further insight into dynein function, we have initiated a structural analysis of individual components of this massive motor complex using NMR spectroscopy. To date, the structures of the motor domain-associated light chain LC1 (Wu et al., 2003; Wu et al., 2000) and the LC8 protein dimer (Fan et al., 2001; Liang et al., 1999) that is found in many multimeric complexes have been solved. In addition, molecular models for the AAA$^+$ domains within the dynein heavy chains have been built (Mocz and Gibbons, 2001 and our unpublished data). Previously, we and others presented the NMR resonance assignments for the *Chlamydomonas* (Wu et al., 2001) and murine (Mok et al., 2001) Tctex1 proteins and defined the overall secondary structure and topology. Furthermore, chemical shift mapping experiments identified residues on Tctex1 that are important for binding the (K/R)(K/R)XX(K/R) motif on the dynein intermediate chain (Mok et al., 2001). However, due to sample aggregation and consequent line broadening of the NOESY spectra, the three-dimensional structure of Tctex1 could not be obtained at that time. Using additional ^{15}N, ^{13}C-labeled samples, we have now obtained those data and report here the high-resolution NMR solution structure for the Tctex1 dimer from *Chlamydomonas* inner dynein arm I1. We demonstrate that this protein exhibits remarkable structural similarity with the LC8 dynein light chain, although the sequences bear no obvious homology with each other. Mapping of residues required for intermediate chain binding onto the molecular surface and analysis of differences between Tctex1 and rp3 suggest a mechanism by which dynein-cargo interactions may be achieved and their specificity defined. Furthermore, this structure provides insight into the consequences of the three mutations present in the *t* haplotype forms of murine Tctex1 that may be involved in transmission ratio distortion.

Results

Solution Structure and Surface Properties of the Tctex1 Dimer

The Tctex1 light chains are components of both cytoplasmic and axonemal dyneins. A sequence alignment between murine and *Chlamydomonas* Tctex1 and the closely related alternate cytoplasmic dynein light chain rp3 is shown in Figure 1. The *Chlamydomonas* inner arm and murine proteins share 60% identity. The secondary structure for *Chlamydomonas* Tctex1 is displayed above the alignment and indicates that this protein consists of a short N-terminal β strand, followed by two α helices and four additional strands in the C-terminal region. The NMR structure of the Tctex1 dimer (total mass = 25,610 Da) is illustrated by the backbone trace display of the 15 lowest energy conformers of the ensemble (Figure 2A) and by the backbone ribbon diagram (Figures 2B and 2C). For residues 4–113 (residues 1–3 and 114 are not well defined), the overall heavy atom backbone root mean square (rms) deviation is 0.76 ± 0.07 Å (0.59 ± 0.06 Å for secondary structure elements). Residues 76–79 are less well defined than other β strand regions. Although we have complete chemical shift assignments for these residues (Wu et al., 2001) and obtained sequential short-range NOEs, no long-range NOEs to the adjacent strand were observed. In contrast, many long-range NOEs were obtained for the upper part of this strand (residues 80–85). Interestingly, the analogous region of the close structural homolog LC8 (see below) also exhibits considerable backbone flexibility (Fan et al., 2002). The structural statistics for Tctex1 are shown in Table 1.

For each Tctex1 monomer, the two long α helices form an anti-parallel hairpin structure packed on a β sheet consisting of five anti-parallel β strands. In this β

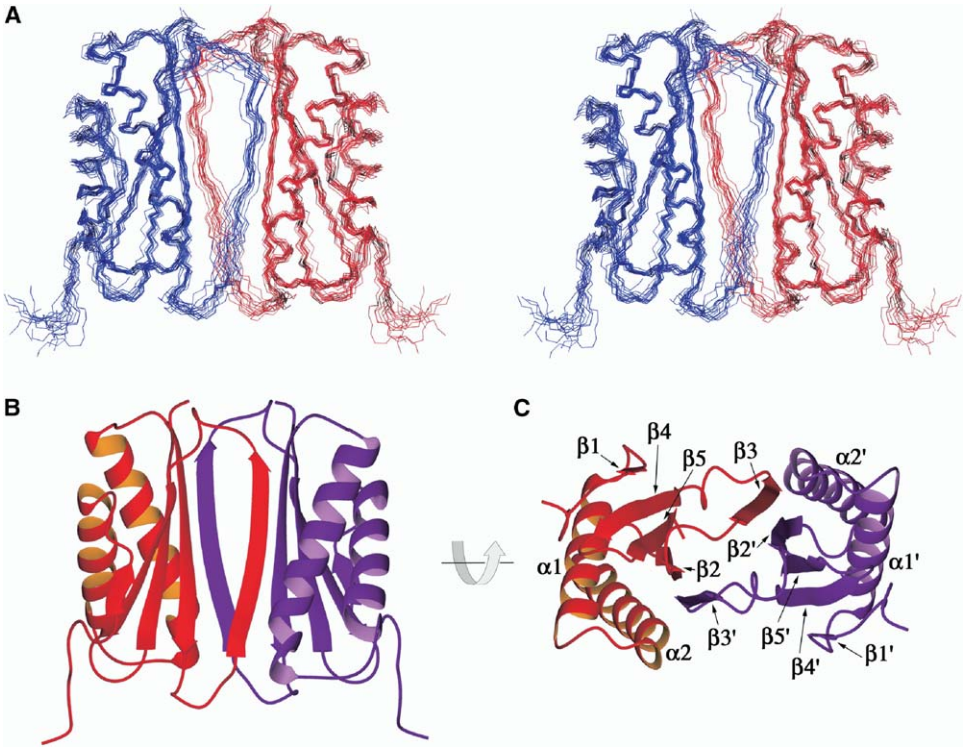

Figure 2. Solution Structure of *Chlamydomonas* Tctex1

(A) Stereo view of the backbone trace for the 15 lowest-energy structures in the final Tctex1 dimer ensemble. The N termini are at the bottom of the display, and the two monomers are colored in red and blue. The backbone rms deviation for residues 4–113 is 0.76 ± 0.07 Å. Residues 1–3 and 114 are not well defined.

(B and C) Two views of the ribbon trace for the Tctex1 dimer related by a 90° rotation about the x axis. The two monomers are colored differently for clarity. The individual secondary structure elements are indicated in (C). Association of the monomers is through two β sheets; in each sheet, four strands derive from one monomer and the fifth from the other monomer. This arrangement forms a strand-switched dimer interface.

sheet, four β strands (β1, β2, β4, and β5) derive from one monomer and the fifth β strand (β3′) from the other monomer. Thus, the two monomers associate across a strand-switched β sheet interface to form a symmetric dimer with two extended shallow grooves. The molecular surface of the Tctex1 dimer is shown in Figure 3. Much of this surface is highly charged and includes both acidic and basic patches on the α-helical surfaces. In addition, there are hydrophobic regions at either end of the grooves formed between the two monomers.

The residues involved in dimer interface formation and the electrostatic properties of this surface are shown in Figures 4A and 4B. These include a series of hydrophobic residues located on strands β2, β3, and β5 as well as two polar residues that are both buried at the interface. Sequence alignment of murine Tctex1 with the alternate mammalian dynein light chain rp3 reveals that four of the eight residues buried at the dimer interface are identical in the two proteins. The other differences represent relatively conservative substitutions (*Chlamydomonas*/mouse Tctex1 → rp3; I/V69 → A, M71 → V, T/S108 → N, and L112 → I using *Chlamydomonas* Tctex1 residue numbers).

Tctex1 Is a Structural Homolog of LC8

The solution structure of Tctex1 revealed a dramatic similarity with the LC8 dynein light chain that is a component of many cellular multimeric complexes, even though these proteins share <17% identity. Both dimeric proteins exhibit the helical hairpin faces and the strand-switched dimer interface. Indeed, the orientation of all secondary structural elements is very similar. The rms deviation for C_α atoms between Tctex1 and LC8 is 2.64 Å, as determined by DALI (Holm and Sander, 1993), indicating that the two structures are closely related; an overlay of the two ribbon diagrams is shown in Figure 5. The major distinction between the two proteins derives from the elongation of Tctex1 by ~10 Å along the axis defined by the intermonomer grooves (an ~40% increase over LC8); these proteins are of very similar dimensions along the other two axes. This results in a significantly larger exposed surface area of 13,485 Å^2 for the Tctex1 dimer versus 9,739 Å^2 for the LC8 dimer. Similarly, the surface area per monomer buried at the interface is increased from 843 Å^2 for LC8 to 1,341 Å^2 for Tctex1; this represents 14.7% and 16.6% of the total monomer surface, respectively.

Importantly, the structure of LC8 has been solved with bound peptides from both neuronal nitric oxide synthase (Fan et al., 2001; Liang et al., 1999) and the proapoptotic factor Bim (Fan et al., 2001). Although the interacting sequences from these two proteins are quite different, both bind in an extended conformation along the entirety of the grooves formed at the LC8 dimer interface. Interaction of both peptides involves hy-

Table 1. Structural Statistics for the Ensemble of 15 Tctex1 Dimer Structures

Rms Deviation (Å) with Respect to Mean	
Residues (4–113)	
Backbone atoms	0.76 ± 0.07
Heavy atoms	1.29 ± 0.16
Secondary structure elements (10–11, 16–32, 37–58, 63–71, 78–85, 93–99, 104–112)	
Backbone atoms	0.59 ± 0.06
Heavy atoms	1.03 ± 0.07
Meaningful Experimental Restraints	
Intraresidue distances per monomer	300
Interresidue distances per monomer	441
Interresidue medium-range distances per monomer	399
Interresidue long-range distances per monomer	348
Intersubunit distances per monomer	93
Hydrogen bond restraints per monomer	54
Dihedral angles per monomer (85 ϕ, 71 ψ, 58 χ_1)	214
Total number of restraints for the dimer	3698
NOE violations[a] >0.3 Å	1.07 ± 1.03
Dihedral angle violations[a] >3°	0.93 ± 1.03
Rms Deviation from Experimental Restraints	
Distance restraints (Å)	0.031 ± 0.002
Dihedral angles (°)	0.592 ± 0.045
Rms Deviation from Idealized Covalent Geometry[b]	
Bonds (Å)	0.004 ± 0.000
Bond angles (°)	0.514 ± 0.016
Improper torsions (°)	0.374 ± 0.021

[a] No distance restraints were violated by >0.5 Å, and no dihedral angles were violated by >5°.
[b] Idealized geometry is defined by the CHARMM force field as implemented within X-PLOR.

drogen bond formation between backbone carbonyls and amides. However, the (K/R)XTQT consensus found in Bim also employs charge-charge interactions, whereas the TGIQV sequence from neuronal nitric oxide synthase involves hydrophobic associations. The LC8 binding motif on the dynein intermediate chain is similar to that of Bim and thus likely interacts in a similar manner (Fan et al., 2001). Combined with the secondary structural and topological similarities between LC8 and Tctex1 reported previously (Wu et al., 2001; Mok et al., 2001), this has led to the presumption that Tctex1 likely also associates with interacting proteins in a manner similar to that observed for LC8.

Tctex1 Molecular Surfaces Involved in Dynein and Cargo Associations

Addition of an 11 residue cytoplasmic dynein intermediate chain peptide (LGRRLHKLGVS), which includes the consensus binding motif, to murine Tctex1 revealed 11 light chain residues for which the chemical shift of the amide proton in the ^{1}H-^{15}N HSQC spectrum changed significantly (Mok et al., 2001) (see Figure 1). This shift is indicative of an alteration in chemical environment upon peptide binding, and consequently defines regions that are likely involved in intermediate chain-light chain interactions. Nine of these residues are completely conserved between *Chlamydomonas* and murine Tctex1; the others represent a conservative substitution W85 → F and a change from hydrophobic to negatively charged A57 → K (see Figure 1).

Mapping these intermediate chain-interacting residues onto the *Chlamydomonas* Tctex1 molecular surface revealed that they do not occur along the intermonomer grooves as is seen with LC8, but rather are all located at one end of the molecule (Figures 6A–6C). The surface of this region exhibits a complex electrostatic potential (Figure 3, upper panel) that includes both charged (K63, D87, D91), polar (T56, C84, T90), and hydrophobic residues (A57, F62, W85, W86), as well as G92 (Figure 6D). Due to the strand-switched dimer interface, these residues form a central polar/charged region bounded by two hydrophobic stripes in which F62 derives from one monomer and W85 and W86 from the second unit (Figures 6D and 4, upper panel). The two alterations between *Chlamydomonas* and murine Tctex1 (A57 → K and W85 → F) occur at the periphery of the region and are indicated in Figure 6E. The analogous region of the rp3 light chain involves several additional alterations when compared to *Chlamydomonas* Tctex1, including T56 → V, F62 → Y, and T90 → S (Figures 1 and 6F).

As Tctex1 and rp3 both bind the dynein intermediate chain yet exhibit distinct cargo binding activities, we examined the molecular surface outside of the intermediate chain binding region to identify differences that may potentially explain the specificity observed for interactions between cargoes and the Tctex1/rp3 dynein proteins. As indicated in Figures 7A and 7B, a number of significant alterations between these two proteins exist; this is also shown with the same color code in the sequence alignment (Figure 1). For example, in both *Chlamydomonas* and murine Tctex1, the Lys residue (K39; K38 in mouse) at the start of the α2 helix and the Tyr (Y104; Y103 in mouse) in the β5 strand are converted

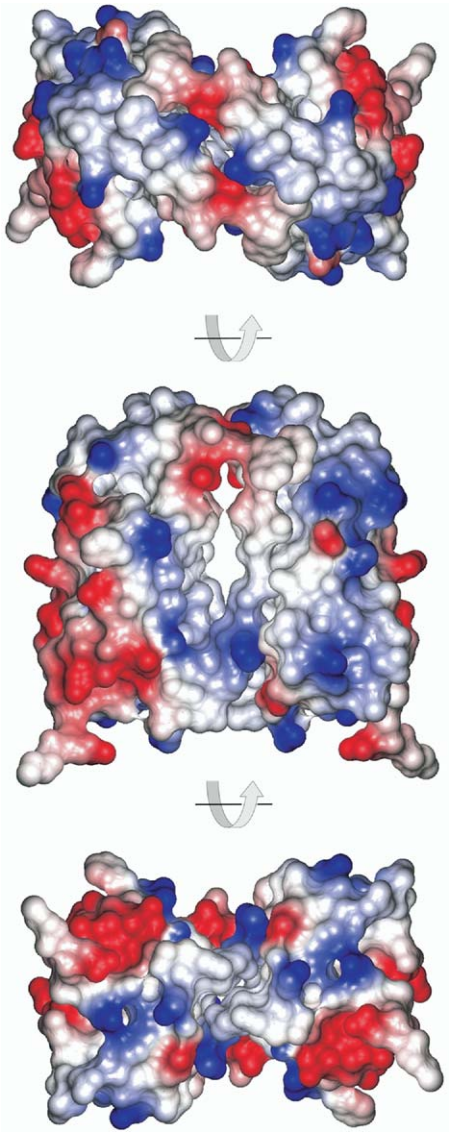

Figure 3. Electrostatic Potential Surface of the Tctex1 Dimer

Three views of the molecular surface of the Tctex1 dimer related by sequential 90° rotations are shown. The center and lower views are in the same orientation as the ribbon diagrams in Figures 2B and 2C, respectively. The surface is colored to reveal the electrostatic properties (blue, positively charged; red, negatively charged). The surface potential was calculated using dielectric constants of 30 and 80 for protein and solvent, respectively.

to Asn in rp3. Moreover, two polar residues (Q33 and Q34) in *Chlamydomonas* Tctex1 (N32 and A33 in the murine version) located in the loop between helices α1 and α2 are changed to acids (E33 and D34) in rp3 (see Figure 1). An additional change, A76 (A75 in mouse) → Y, which is located at the base of the intermonomer grooves, will lead to increased hydrophobicity in this section of rp3. With the exception of T108 (S107 in mouse) → N in rp3, which is located in the center of the intermonomer grooves, all these changes occur far from the intermediate chain binding region at the opposite end of the molecule and in general involve only the very periphery of the grooves.

Location of the *t* Haplotype Mutations within Tctex1

Tctex1 is a candidate for the proximal distorter/sterility factor involved in non-Mendelian transmission of the murine *t* haplotype (Lader et al., 1989). Compared to the wild-type *t* complex forms, *t* haplotype-encoded Tctex1 variants contain three amino acid substitutions that might alter Tctex1 activity/function (see Figure 1). Two of these changes (Q → H and L → I) occur within the α2 helix on the walls of the intermonomer grooves, whereas the third (R → K) is located in the loop between α2 and the β2 strand and is immediately adjacent to the intermediate chain binding region (Figures 7C and 7D). The Arg-to-Lys transition is unlikely to be significant, as both *Chlamydomonas* Tctex1 and human rp3 have a Lys residue in this position. Likewise, the Leu-to-Ile alteration represents a very conservative substitution, and, moreover, the side chain of this residue is partly buried. In contrast, Q42 (using the *Chlamydomonas* numbering) is completely conserved from algae to humans and is exposed at the edge of the intermonomer grooves.

Discussion

Here, we have used multidimensional NMR spectroscopic methods to determine the solution structure of the Tctex1 light chain dimer from *Chlamydomonas* inner dynein arm I1. This represents only the second high-resolution structure determined for a dynein-specific component. Previously, the structure of the dynein motor domain-associated, leucine-rich repeat protein LC1 was solved. Structural data are also available for LC8, which is present in many multimeric complexes and is not dynein specific. The considerable structural homology of Tctex1 with LC8, and localization of residues involved in dynein intermediate chain binding that are mutated in the *t* haplotype variants, provides insight into the mechanisms and specificity of dynein-cargo interactions.

Structural Implications for the Interaction of Tctex1 with Dynein and Cargo Proteins

Within each cytoplasmic dynein complex, there are two copies of the IC74 intermediate chain (King et al., 1998) as well as two copies of Tctex1 (King et al., 1996b) and LC8 (King et al., 1996a). Previously, it has been proposed that LC8 binds both dynein and cargo proteins via the intermonomer grooves (presumably with one groove bound to dynein and the other to cargo). However, there is a problem with this scenario in that it leaves an unsatisfied LC8 binding site on one of the dynein intermediate chains. Likewise, the prediction that Tctex1 binds the intermediate chain via the grooves leads to the same inherent predicament. Also, if the dynein and cargo binding surfaces are the same, there is the added question of how Tctex1 and rp3 can both bind the intermediate chain but not the same cargo.

Although LC8 has been shown to be a component of both axonemal and cytoplasmic dyneins (King et al., 1996a; King and Patel-King, 1995; Pfister et al., 1982), this protein also binds a wide variety of different cellular proteins—e.g., myosin V (Espindola et al., 2000), neu-

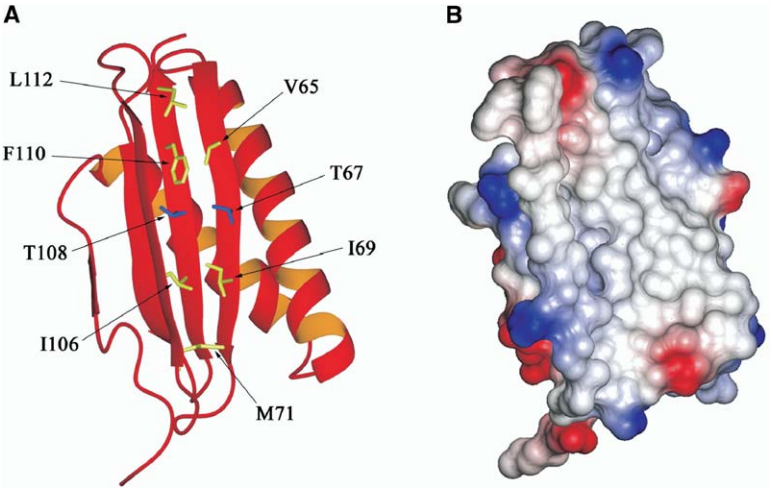

Figure 4. The Intermonomer Interface of Tctex1

(A and B) A ribbon diagram of one monomer of the Tctex1 dimer is shown in (A), and the corresponding molecular surface (much of which is buried in the dimer structure) is shown in panel (B). The polar (blue) and hydrophobic (yellow) residues buried following intermonomer interactions are indicated. This interface is mainly hydrophobic, but it also includes two polar residues. The molecular surface is colored to reveal the electrostatic properties (blue, positively charged; red, negatively charged).

ronal nitric oxide synthase (Jaffrey and Snyder, 1996), Bim (Puthalakath et al., 1999), and many others. Indeed, ~80% of brain LC8 is not dynein associated (King et al., 1996a). Moreover, there is no compelling evidence to demonstrate that an LC8 dimer actually binds cargoes directly to dynein, although this is the interpretation that has been often put forward. An equally plausible scenario is that LC8 is simply an essential part of many multiprotein complexes (perhaps employed as intermolecular "glue"), but does not mediate dynein-cargo interactions per se. In contrast, there is strong evidence supporting the direct association of a cargo (namely, rhodopsin [Tai et al., 1999, 2001]) with dynein via Tctex1; importantly, rhodopsin does not interact with the Tctex1 homolog rp3. The structural work on Tctex1 reported here, combined with chemical shift mapping experiments published previously (Mok et al., 2001), provides for an alternative mechanism of light chain-mediated dynein-cargo interactions that also can explain the cargo binding specificity exhibited by Tctex1 compared with rp3.

The diagram shown in Figure 8A illustrates the segment of Tctex1 that is involved in association with the dynein intermediate chain and reveals that much of the molecule, including most of the intermonomer grooves, would be available to bind a specific cargo without affecting the dynein binding region. Although both Tctex1 and rp3 bind the dynein intermediate chain, the exposed region available to interact with cargo contains several residues that are different between the two light chain isoforms; these alterations would result in dramatically different electrostatic/hydrophobic surface properties. These surface alterations are likely more than sufficient to explain the observed differences between these two molecules (i.e., Tctex1 can bind rhodopsin, while rp3 cannot [Tai et al., 2001]). In contrast, the structurally related LC8 protein, which associates with the dynein intermediate chain immediately C-terminal to the Tctex1 binding region, interacts with its target peptides along the entire intermonomer cleft (Figure 8B). In order for this protein to act as a dynein cargo adaptor, one of the two intermediate chains would need to be displaced from this binding surface.

The chemical shift mapping experiments with Tctex1 reported by Mok et al. (Mok et al., 2001) employed an 11-residue dynein intermediate chain peptide containing the (K/R)(K/R)XX(K/R) motif that they found to be essential for association of these two proteins. However, this peptide was not sufficient for high-affinity interaction with Tctex1, as measured with a fusion protein pull-down assay. This observation suggested that an additional interaction involving another part of the 19-residue Tctex1 binding domain might be required. More recently, following further sequence analysis, a second Tctex1 binding motif VS(K/H)(T/S)X(V/T)(T/S)(N/Q)V that may be important has been proposed, although gaps

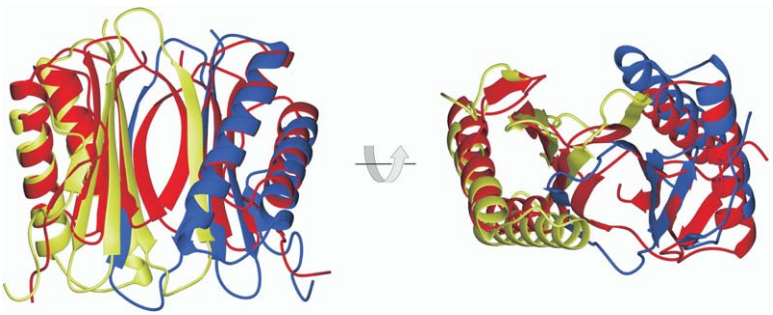

Figure 5. Tctex1 Is a Structural Homolog of the LC8 Dynein Light Chain

Two views (related by a 90° rotation) of the superimposed ribbon structures for *Chlamydomonas* Tctex1 (monomers are colored yellow and blue) and rat LC8 (PDB accession 1F95; both monomers are red) are shown. The rms deviation for superimposed C_α atoms is 2.64 Å, as determined by DALI (Holm and Sander, 1993). Although apparently unrelated at the primary sequence level, this comparison reveals the close structural homology between these two dynein components; the major difference derives from an ~10 Å elongation of Tctex1 along the axis defined by the intermonomer grooves.

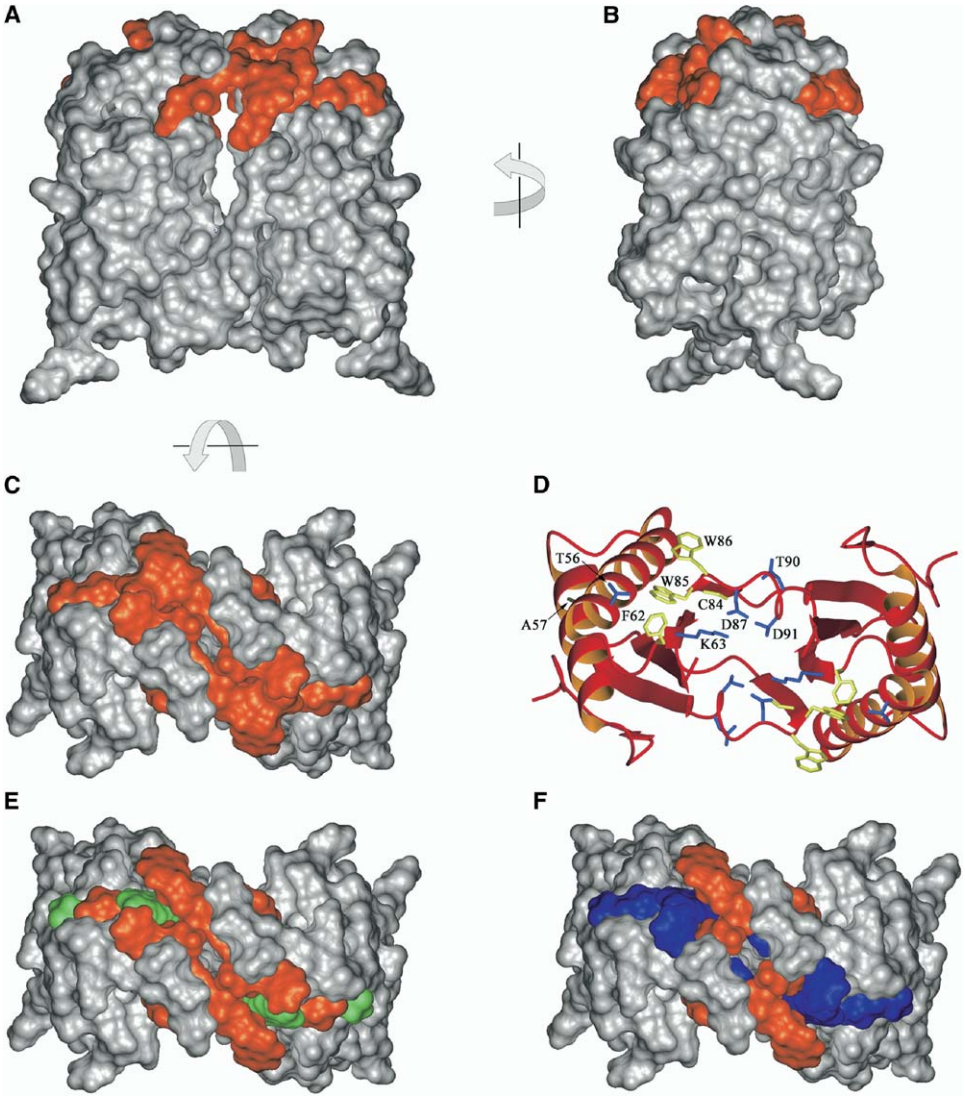

Figure 6. Location and Properties of Interaction Surfaces on Tctex1

(A–C) Three views of the *Chlamydomonas* Tctex1 molecular surface in which the residues of murine Tctex1 that show alterations in chemical shift upon binding of a dynein intermediate chain peptide are colored orange (T56, A57, F62, K63, C84, W85, W86, D87, T90, D91, and G92 in the *Chlamydomonas* protein). These residues cluster to one end of the structure and extend only part way into the intermonomer grooves.

(D) Ribbon diagram of Tctex1 on which the residues involved in intermediate chain binding are indicated (blue, polar or charged; yellow, hydrophobic); residues are identified on only one monomer. The orientation is as in (C).

(E and F) Residues involved in binding the intermediate chain peptide that are different between ([E], green) *Chlamydomonas* and murine Tctex1 and ([F], blue) *Chlamydomonas* Tctex1 and human rp3 are indicated. Identical residues are shown in orange.

of varying length need be inserted and parts are missing in various Tctex1 binding proteins (Sugai et al., 2003). Interestingly, part of this motif ($_{337}$***VSK***TE***TSQ V***APA$_{348}$) is present in the C-terminal tail of rhodopsin (which lacks the basic motif discussed above) and includes one of the two mutations (V345M) that reduce affinity for Tctex1 and result in *retinitis pigmentosa* (Tai et al., 1999) (a second mutation occurs at P347). Previously, several other Tctex1-interacting proteins have been described, including Doc-2 (Nagano et al., 1998) and the CD5 receptor (Bauch et al., 1998), that contain the same basic binding motif as the dynein intermediate chain; however, these proteins lack the second motif proposed by Sugai et al. (2003) (the CD155 poliovirus receptor [Mueller et al., 2002] also exhibits only very weak homology to this second motif). Thus, unlike rhodopsin, these proteins must presumably interact with the same region of Tctex1 as the intermediate chain. Given the small size of this interaction surface, it is unlikely that both dynein and cargo could be bound at the same time due to steric considerations, unless one dynein intermediate chain was displaced. Consequently, it becomes uncertain as to whether these molecules could be tethered to, and thus transported by, dynein via an interaction with Tctex1.

Can Tctex1 and rp3 Form a Heterodimer?

As members of the Tctex1 light chain family apparently mediate interaction of the dynein motor with specific cellular cargoes, different dynein particles likely display

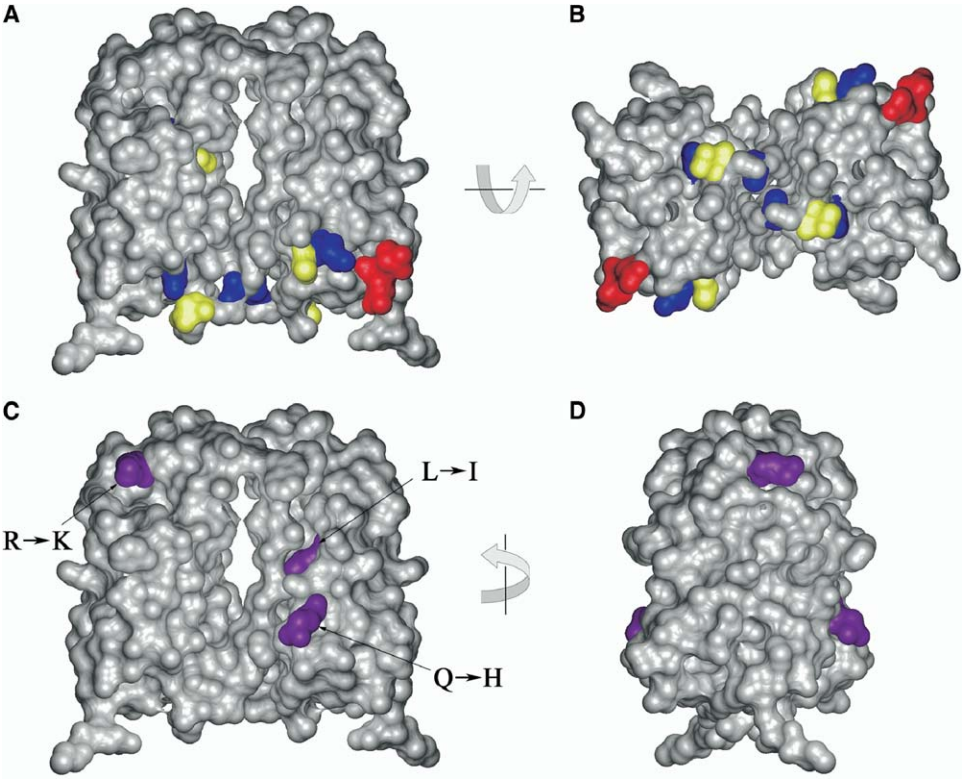

Figure 7. Surface Variations in Tctex1-like Proteins and the Location of *t* Haplotype-Encoded Mutations

(A and B) Two views of the molecular surface colored to identify several residues outside of the intermediate chain binding region that are significantly different between Tctex1 and rp3: red, polar to negatively charged; yellow, semiconservative substitutions; blue, significant alteration in hydrophobicity or hydrophilicity (color code is as in Figure 1).

(C and D) The three residues that are mutated in the *t* haplotype forms of murine Tctex1 are indicated (in purple) on the molecular surface of the *Chlamydomonas* protein.

distinct cargo binding properties depending on their light chain content. As Tctex1 and rp3 are differentially expressed, certain tissues in which one isoform is significantly overexpressed compared to the other (e.g., fetal and adult brain, which are highly enriched for Tctex1 and rp3, respectively [DiBella et al., 2001; Roux et al., 1994]) should contain dyneins containing only rp3 or Tctex1 light chain homodimers. However, in tissues in which both isoforms are expressed in relatively equal amounts (e.g., adult liver and kidney), cargo binding diversity might be increased if certain dynein particles contain a Tctex1/rp3 heterodimer. Analysis of the Tctex1 dimer interface revealed that many of the residues involved in intermonomer interactions are conserved between the two isoforms; the remaining differences represent conservative substitutions. Within the intermonomer region, rp3 protein only differs significantly from Tctex1 at a single residue located at the periphery of the interface. Thus, there does not appear to be any essential structural impediment to heterodimer formation. This is consistent with recent yeast two-hybrid results, which indicate a robust interaction between Tctex1 and rp3 (Lo et al., 2004).

Structural Consequence of the *t* Haplotype-Encoded Mutations in Tctex1

The murine *t* haplotypes represent a 30–40 Mb region of chromosome 17 that contains a series of inversions that suppress recombination with the wild-type *t* complex. Transmission ratio distortion results in heterozygous males passing the *t* haplotype form of chromosome 17 to >95% of their progeny (Lyon, 2003). This effect occurs through defects in spermiogenesis such that sperm carrying the wild-type copy of this chromosome are compromised in their ability to reach and/or fertilize the oocyte. It is remarkable that this genomic rearrangement has survived at high levels in feral populations, as homozygosity for a particular *t* haplotype is fatal due to the presence of a series of recessive lethal factors. Even in the hemizygous state (i.e., homozygous mice that carry complementing *t* haplotypes with different recessive lethals), males are sterile due to homozygosity for several sterility factors. This phenomenon is thought from genetic evidence to be caused by the action of a responder on several distorters (Lyon, 1984). Candidates for distorters include Tctex1 (Lader et al., 1989), Tctex2 (Huw et al., 1995), and a dynein heavy chain (Dnahc8) encoded at the *Hybrid Sterility 6* locus that appears to be the mammalian equivalent of the *Chlamydomonas* outer arm γ heavy chain (Samant et al., 2002). Interestingly, in *Drosophila*, lack of Tctex1 results in male sterility but does not lead to obvious deficiencies in cytoplasmic dynein function (Caggese et al., 2001; Li et al., 2004). The responder has been identified as a sperm motility kinase (Smok); the *t* haplotype version (Tcr^t) has abrogated catalytic func-

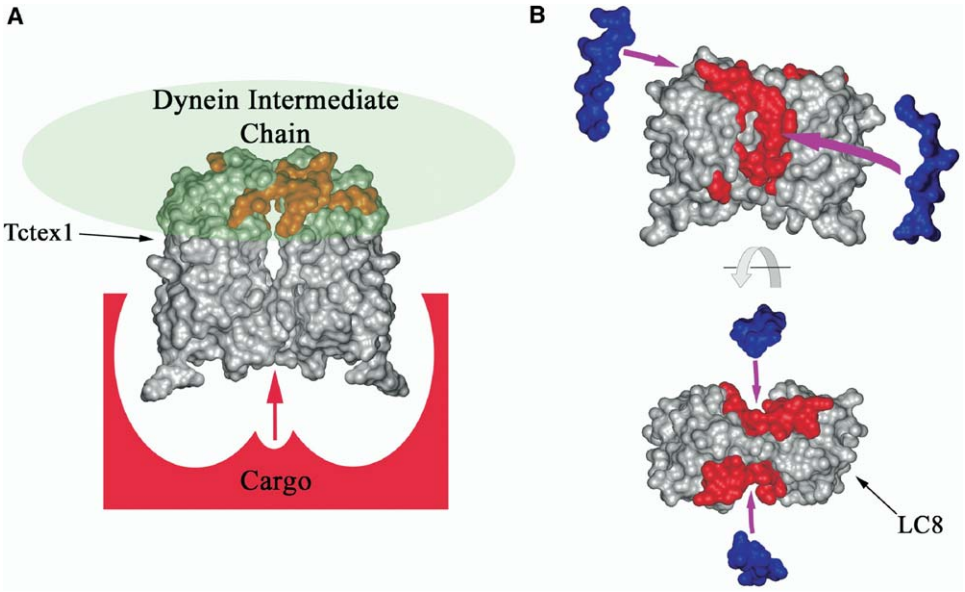

Figure 8. Model for Dynein-Cargo Interactions Mediated by Tctex1

(A) Model for the interaction surfaces of Tctex1 involved in dynein intermediate chain and cargo binding. Chemical shift mapping data indicate that association with the intermediate chain (K/R)(K/R)XX(K/R) motif involves the upper portion of the Tctex1 dimer. This would then allow cargo proteins (such as rhodopsin) to bind the opposite region using a different chemical mechanism. The advantages of this model include 1) that dynein and cargo associate via distinct mechanisms, 2) that unsatisfied Tctex1 binding sites need not be exposed on the dynein particle following cargo attachment, and 3) that alterations in the molecular surface of rp3 versus Tctex1 can explain the observation that both proteins bind dynein intermediate chain, but only Tctex1 interacts with rhodopsin.

(B) Interaction of the structurally related LC8 dimer with peptides from multiple distinct proteins (including neuronal nitric oxide synthase, Bim, and dynein intermediate chain; the Bim peptides are shown in blue) involves the entirety of the intermonomer grooves (indicated in red on the molecular surface). If this protein in fact acts as a dynein-cargo adaptor, both components must bind in a similar manner, displace an intermediate chain, and leave an unsatisfied LC8 binding region on the dynein particle.

tion due to fusion with a second kinase (Herrmann et al., 1999).

Current models (Harrison et al., 1998; Pazour et al., 1999) suggest that *t* haplotype-encoded mutations in the distorters lead to formation of poisonous products, potentially following phosphorylation by wild-type Smok, but that these same mutations result in protection from the detrimental action of Tcr^t. If Tctex1 is indeed a distorter, the *t* mutations might then be predicted to alter the ability of this protein to be phosphorylated. Interestingly, related proteins in sea urchin and fish sperm are phosphorylated upon the acquisition of the ability to swim (Inaba et al., 1999), although it is unknown whether the murine protein is similarly modified. Structural analysis of the three *t* haplotype-specific mutations in murine Tctex1 reveals that two (R → K and L → I) are unlikely to be of significance. The R → K change is directly adjacent to the dynein intermediate chain binding region, and, indeed, this alteration also is present in rp3 and *Chlamydomonas* Tctex1; the L → I transition occurs at a position that is mostly buried near the base of the intermonomer grooves. In contrast, Q → H alters a highly conserved residue that is exposed at the surface of the α2 helix near the grooves. Intriguingly, in murine Tctex1, this residue immediately adjoins an exposed Thr (S45 in *Chlamydomonas*) that represents a potential target for Smok.

In conclusion, we demonstrate that Tctex1 is a close structural homolog of the LC8 dynein light chain and contains a strand-switched dimer interface. The Tctex1 solution structure and previously reported chemical shift mapping data (Mok et al., 2001) allow the dynein intermediate chain binding region to be identified. Furthermore, this structure provides intriguing insight into the mechanisms by which dynein motors interact with cargo and how those associations might be specified. Examination of the mutations that occur in the *t* haplotype forms of Tctex1 allows predictions to be made concerning their consequences for non-Mendelian chromosome transmission.

Experimental Procedures

Protein Purification

The ^{15}N, ^{13}C-labeled *Chlamydomonas* Tctex1 protein from inner dynein arm I1 was expressed with an N-terminal His_{10} tag by using the pET23d vector in *Escherichia coli* strain BL21(DE3) grown in ^{15}N, ^{13}C BioExpress 1000 medium (Cambridge Isotope Laboratories Inc., Andover, MA). Following purification by Ni^{2+} affinity chromatography, the tag was removed by digestion with factor Xa, leaving a single additional His residue at the N terminus. ^{15}N, ^{13}C-labeled Tctex1 samples were concentrated to ~0.7 mM in a volume of 250 μl. The protein was exchanged into 20 mM Na phosphate (pH 6.7), 100 mM NaCl, 20 mM dithiothreitol in 90% H_2O/10% D_2O. For HCCH-TOCSY and ^{13}C HSQC-NOESY experiments, the protein was exchanged into >99% D_2O.

NMR Spectroscopy

Details of the NMR experiments have been described previously (Wu et al., 2001). All data were collected at 25°C on four-channel Varian INOVA 600 or INOVA 500 spectrometers using pulse-field gradient triple resonance probes. The data were processed with

NMRPipe (Delaglio et al., 1995) and were analyzed with the program XEASY (Bartels et al., 1995).

Structure Determination

Intramonomer distance restraints were obtained from the three-dimensional ^{15}N NOESY-HSQC (τ = 150 ms) and ^{13}C HSQC-NOESY (τ = 150 ms) spectra. Intermonomer distance restraints were obtained from ^{13}C three-dimensional edited/filtered NOESY (Zwahlen et al., 1997) (τ = 200 ms) and ^{15}N two-dimensional edited/filtered NOESY (τ = 200 ms) spectra with a sample containing ~0.5 mM ^{15}N, ^{13}C-labeled Tctex1 and ~0.5 mM unlabeled Tctex1. Based on these two spectra, a total of 93 intermonomer (78 side chain and 15 backbone) NOE constraints were identified. The upper bounds for interproton distances were calibrated from the NOEs with CALIBA (Güntert et al., 1997). Initially, sequential NOEs and unambiguous long-range NOEs were identified. Multiple initial structure calculations were performed with the program CYANA (Güntert et al., 1997). Additional long-range NOE assignments were made with the program CANDID (Herrmann et al., 2002) and were manually checked. The ϕ and ψ backbone torsion angles were predicted with the program TALOS (Cornilescu et al., 1999). Side chain χ_1 angles were assigned based on intraresidue NOE patterns. Slowly exchanging amide protons were used in the evaluation of hydrogen bonds. For the hydrogen-deuterium exchange experiments, the Tctex1 protein sample was dialyzed directly into buffer made in 99.9% D_2O. The K60-P61 peptide bond is *cis*, as determined from sequential $d_{\alpha i-\alpha(i+1)}$ NOEs between Lys 60 and Pro 61. Using a complete set of NOEs, dihedral, and hydrogen bond restraints, 600 structural conformers were calculated in CYANA, and 90 of those with the lowest target function were refined in X-PLOR (Brunger, 1992). Fifteen structures were selected on the basis of a minimal number of restraint violations as given in Table 1. Structures were displayed with MOLMOL (Koradi et al., 1996).

Acknowledgments

This study was supported by grants GM51293 (NMR assignments) and GM63548 (structure determination) from the National Institutes of Health. S.M.K. is an investigator of the Patrick and Catherine Weldon Donaghue Medical Research Foundation.

Received: October 4, 2004
Revised: November 10, 2004
Accepted: November 15, 2004
Published: February 8, 2005

References

Afzelius, B.A. (1979). The immotile-cilia syndrome and other ciliary diseases. Int. Rev. Exp. Pathol. *19*, 1–43.

Bartels, C., Xia, T., Billeter, M., Güntert, P., and Wüthrich, K. (1995). The program XEASY for computer supported NMR spectral-analysis of biological macromolecules. J. Biomol. NMR *6*, 1–10.

Bauch, A., Campbell, K.S., and Reth, M. (1998). Interaction of the CD5 cytoplasmic domain with the Ca^{2+}/calmodulin- dependent kinase IIδ. Eur. J. Immunol. *28*, 2167–2177.

Brunger, A.T. (1992). X-PLOR: a system for X-ray crystallography and NMR (New Haven, CT: Yale University Press).

Caggese, C., Moschetti, R., Ragone, G., Barsanti, P., and Caizzi, R. (2001). *dtctex-1*, the *Drosophila melanogaster* homolog of a putative murine *t*-complex distorter encoding a dynein light chain, is required for production of functional sperm. Mol. Genet. Genomics *265*, 436–444.

Cornilescu, G., Delaglio, F., and Bax, A. (1999). Protein backbone angle restraints from searching a database for chemical shift and sequence homology. J. Biomol. NMR *13*, 289–302.

Delaglio, F., Grzesiek, S., Vuister, G., Zhu, G., Pfeifer, J., and Bax, A. (1995). NMRPipe: a multidimensional spectral processing system based on UNIX pipes. J. Biomol. NMR *6*, 277–293.

DiBella, L.M., Benashski, S.E., Tedford, H.W., Harrison, A., Patel-King, R.S., and King, S.M. (2001). The Tctex1/Tctex2 class of dynein light chains. Dimerization, differential expression, and interaction with the LC8 protein family. J. Biol. Chem. *276*, 14366–14373.

Douglas, M., Diefenbach, R., Homa, F., Miranda-Saksena, M., Rixon, F., Vittone, V., Byth, K., and Cunnungham, A. (2004). *Herpes simplex* virus type 1 capsid protein VP26 interacts with dynein light chains rp3 and Tctex1 and plays a role in retrograde cellular transport. J. Biol. Chem. *279*, 28522–28530.

Espindola, F.S., Suter, D.M., Partata, L.B., Cao, T., Wolenski, J.S., Cheney, R.E., King, S.M., and Mooseker, M.S. (2000). The light chain composition of chicken brain myosin-Va: calmodulin, myosin-II essential light chains, and 8-kDa dynein light chain/PIN. Cell Motil. Cytoskeleton *47*, 269–281.

Fan, J.-S., Zhang, Q., Tochio, H., Li, M., and Zhang, M. (2001). Structural basis of diverse sequence-dependent target recognition by the 8 kDa dynein light chain. J. Mol. Biol. *306*, 97–108.

Fan, J.S., Zhang, Q., Tochio, H., and Zhang, M. (2002). Backbone dynamics of the 8 kDa dynein light chain dimer reveals molecular basis of the protein's functional diversity. J. Biomol. NMR *23*, 103–114.

Fossella, J., Samant, S.A., Silver, L.M., King, S.M., Vaughan, K.T., Olds-Clarke, P., Johnson, K.A., Mikami, A., Vallee, R.B., and Pilder, S.H. (2000). An axonemal dynein at the *Hybrid Sterility 6* locus: implications for *t* haplotype-specific male sterility and the evolution of species barriers. Mamm. Genome *11*, 8–15.

Güntert, P., Mumenthaler, C., and Wüthrich, K. (1997). Torsion angle dynamics for NMR structure calculation with the new program DYANA. J. Mol. Biol. *273*, 283–298.

Hafezparast, M., Klocke, R., Ruhrberg, C., Marquardt, A., Ahmad-Annuar, A., Bowern, S., Lalli, G., Witherden, A., Hummerich, H., Nicholson, S., et al. (2003). Mutations in dynein link motor neuron degeneration to defects in retrograde transport. Science *300*, 808–812.

Harrison, A., Olds-Clarke, P., and King, S.M. (1998). Identification of the *t* complex-encoded cytoplasmic dynein light chain Tctex1 in inner arm I1 supports the involvement of flagellar dyneins in meiotic drive. J. Cell Biol. *140*, 1137–1147.

Herrmann, B.G., Koschorz, B., Wertz, K., McLaughlin, J., and Kispert, A. (1999). A protein kinase encoded by the *t* complex responder gene causes non-Mendelian inheritance. Nature *402*, 141–146.

Herrmann, T., Güntert, P., and Wüthrich, K. (2002). Protein NMR structure determination with automated NOE assignment using the new software CANDID and the torsion angle dynamics algorithm DYANA. J. Mol. Biol. *319*, 209–227.

Holm, L., and Sander, C. (1993). Protein structure comparison by alignment of distance matrices. J. Mol. Biol. *233*, 123–138.

Huw, L.Y., Goldsborough, A.S., Willison, K., and Artzt, K. (1995). Tctex2: a sperm tail surface protein mapping to the *t*-complex. Dev. Biol. *170*, 183–194.

Inaba, K., Kagami, O., and Ogawa, K. (1999). Tctex2-related outer arm dynein light chain is phosphorylated at activation of sperm motility. Biochem. Biophys. Res. Commun. *256*, 177–183.

Jaffrey, S.R., and Snyder, S.H. (1996). PIN: an associated protein inhibitor of neuronal nitric oxide synthase. Science *274*, 774–777.

Kagami, O., Gotoh, M., Makino, Y., Mohri, H., Kamiya, R., and Ogawa, K. (1998). A dynein light chain of sea urchin sperm flagella is a homolog of mouse Tctex *1*, which is encoded by a gene of the *t* complex sterility locus. Gene *211*, 383–386.

Kai, N., Mishina, M., and Yagi, T. (1997). Molecular cloning of Fyn-associated molecules in the mouse central nervous system. J. Neurosci. Res. *48*, 407–424.

King, S.M. (2002). Dynein Motors: structure, mechanochemistry and regulation. In Molecular Motors, M. Schliwa, ed. (Weinheim, Germany: Wiley-VCH Verlag GmbH), pp. 45–78.

King, S.M., and Patel-King, R.S. (1995). The $M_{(r)}$ = 8,000 and 11,000 outer arm dynein light chains from *Chlamydomonas* flagella have cytoplasmic homologues. J. Biol. Chem. *270*, 11445–11452.

King, S.M., Barbarese, E., Dillman, J.F., Patel-King, R.S., Carson,

J.H., and Pfister, K.K. (1996a). Brain cytoplasmic and flagellar outer arm dyneins share a highly conserved M_r 8,000 light chain. J. Biol. Chem. *271*, 19358–19366.

King, S.M., Dillman, J.F., 3rd, Benashski, S.E., Lye, R.J., Patel-King, R.S., and Pfister, K.K. (1996b). The mouse *t*-complex-encoded protein Tctex-1 is a light chain of brain cytoplasmic dynein. J. Biol. Chem. *271*, 32281–32287.

King, S.M., Barbarese, E., Dillman, J.F., Benashski, S.E., Do, K.T., Patel-King, R.S., and Pfister, K.K. (1998). Cytoplasmic dynein contains a family of differentially expressed light chains. Biochemistry *37*, 15033–15041.

Koradi, R., Billeter, M., and Wüthrich, K. (1996). MOLMOL: a program for display and analysis of macromolecular structures. J. Mol. Graph. *14*, 51–55.

Lader, E., Ha, H.S., O'Neill, M., Artzt, K., and Bennett, D. (1989). *tctex-1*: a candidate gene family for a mouse *t* complex sterility locus. Cell *58*, 969–979.

Li, M.-g., Serr, M., Newman, E., and Hays, T. (2004). The *Drosophila* Tctex-1 light chain is dispensable for essential cytoplasmic dynein functions but is required during spermatid differentiation. Mol. Biol. Cell *15*, 3005–3014.

Liang, J., Jaffrey, S.R., Guo, W., Snyder, S.H., and Clardy, J. (1999). Structure of the PIN/LC8 dimer with a bound peptide. Nat. Struct. Biol. *6*, 735–740.

Lo, K., Kogoy, J., King, S., and Pfister, K. (2004). Association of the intermediate chains and light chains in the cytoplasmic dynein complex. Mol. Biol. Cell *15*, 564.

Lyon, M. (2003). Transmission ratio distortion in mice. Annu. Rev. Genet. *37*, 393–408.

Lyon, M.F. (1984). Transmission ratio distortion in mouse *t* haplotypes is due to multiple distorter genes acting on a responder locus. Cell *37*, 621–628.

Mocz, G., and Gibbons, I.R. (2001). Model for the motor component of dynein heavy chain based on homology to the AAA family of oligomeric ATPases. Structure *9*, 93–103.

Mok, Y.-K., Lo, K.W.-H., and Zhang, M. (2001). Structure of Tctex-1 and its interaction with cytoplasmic dynein intermediate chain. J. Biol. Chem. *276*, 14067–14074.

Mou, T., Kraas, J.R., Fung, E.T., and Swope, S.L. (1998). Identification of a dynein molecular motor component in *Torpedo* electroplax; binding and phosphorylation of Tctex-1 by Fyn. FEBS Lett. *435*, 275–281.

Mueller, S., Cao, X., Welker, R., and Wimmer, E. (2002). Interaction of the poliovirus receptor CD155 with the dynein light chain Tctex-1 and its implication for poliovirus pathogenesis. J. Biol. Chem. *277*, 7897–7904.

Nagano, F., Orita, S., Sasaki, T., Naito, A., Sakaguchi, G., Maeda, M., Watanabe, T., Kominami, E., Uchiyama, Y., and Takai, Y. (1998). Interaction of Doc2 with Tctex-1, a light chain of cytoplasmic dynein. Implication in dynein-dependent vesicle transport. J. Biol. Chem. *273*, 30065–30068.

O'Neill, M.J., and Artzt, K. (1995). Identification of a germ-cell-specific transcriptional repressor in the promoter of Tctex-1. Development *121*, 561–568.

Patel-King, R.S., Benashski, S.E., Harrison, A., and King, S.M. (1997). A *Chlamydomonas* homologue of the putative murine *t* complex distorter Tctex-2 is an outer arm dynein light chain. J. Cell Biol. *137*, 1081–1090.

Pazour, G.J., Koutoulis, A., Benashski, S.E., Dickert, B.L., Sheng, H., Patel-King, R.S., King, S.M., and Witman, G.B. (1999). LC2, the *Chlamydomonas* homologue of the *t* complex-encoded protein Tctex2, is essential for outer dynein arm assembly. Mol. Biol. Cell *10*, 3507–3520.

Pfister, K.K., Fay, R.B., and Witman, G.B. (1982). Purification and polypeptide composition of dynein ATPases from *Chlamydomonas* flagella. Cell Motil. *2*, 525–547.

Puthalakath, H., Huang, D.C., O'Reilly, L.A., King, S.M., and Strasser, A. (1999). The proapoptotic activity of the Bcl-2 family member Bim is regulated by interaction with the dynein motor complex. Mol. Cell *3*, 287–296.

Roux, A.-F., Rommens, J., McDowell, C., Anson-Cartwright, L., Bell, S., Schappert, K., Fishman, G.A., and Musarella, M. (1994). Identification of a gene from Xp21 with similarity to the *tctex-1* gene of the murine *t* complex. Hum. Mol. Genet. *3*, 257–263.

Sakato, M., and King, S.M. (2004). Design and regulation of the AAA^+ microtubule motor dynein. J. Struct. Biol. *146*, 58–71.

Samant, S., Ogunkua, O., Hui, L., Fossella, J., and Pilder, S. (2002). The *t* complex distorter 2 candidate gene, *Dnahc8*, encodes at least two testis-specific axonemal dynein heavy chains that differ extensively at their amino and carboxyl termini. Dev. Biol. *250*, 24–43.

Schwarzer, C., Barnikol-Watanabe, S., Thinnes, F.P., and Hilschmann, N. (2002). Voltage-dependent anion-selective channel (VDAC) interacts with the dynein light chain Tctex1 and the heat-shock protein PBP74. Int. J. Biochem. Cell Biol. *34*, 1059–1070.

Sugai, M., Saito, M., Sukegawa, I., Katsushima, Y., Kinouchi, Y., Nakahata, N., Shimosegawa, T., Yanagisawa, T., and Sukegawa, J. (2003). PTH/PTH-related protein receptor interacts directly with Tctex-1 through its C-terminal domain. Biochem. Biophys. Res. Commun. *311*, 24–31.

Tai, A.W., Chuang, J.Z., Bode, C., Wolfrum, U., and Sung, C.H. (1999). Rhodopsin's carboxy-terminal cytoplasmic tail acts as a membrane receptor for cytoplasmic dynein by binding to the dynein light chain Tctex-1. Cell *97*, 877–887.

Tai, A.W., Chuang, J.Z., and Sung, C.H. (2001). Cytoplasmic dynein regulation by subunit heterogeneity and its role in apical transport. J. Cell Biol. *153*, 1499–1509.

Wu, H., Maciejewski, M.W., Marintchev, A., Benashski, S.E., Mullen, G.P., and King, S.M. (2000). Solution structure of a dynein motor domain associated light chain. Nat. Struct. Biol. *7*, 575–579.

Wu, H., Maciejewski, M.W., Benashski, S.E., Mullen, G.P., and King, S.M. (2001). ^1H, ^{15}N and ^{13}C resonance assignments for the Tctex1 dynein light chain from *Chlamydomonas* flagella. J. Biomol. NMR *20*, 89–90.

Wu, H., Blackledge, M., Maciejewski, M.W., Mullen, G.P., and King, S.M. (2003). Relaxation-based structure refinement and backbone molecular dynamics of the dynein motor domain-associated light chain. Biochemistry *42*, 57–71.

Zwahlen, C., Legault, P., Vincent, S., Greenblatt, J., Konrat, R., and Kay, L. (1997). Methods for measurement of intermolecular NOEs by multinuclear NMR spectroscopy: application to a bacteriophage N-peptide/boxB RNA complex. J. Am. Chem. Soc. *119*, 6711–6721.

Accession Numbers

The coordinates for the ensemble of Tctex1 structures have been deposited in the Protein Data Bank (accession number 1XDX). The NMR experimental data and chemical shift assignments were reported previously (Wu et al., 2001) and may be obtained from the BioMagResBank (http://www.bmrb.wisc.edu) under accession number 4929.